Vav1 regulates T cell activation through a feedback mechanism and crosstalk between the T cell receptor and CD28

Ynes A. Helou[†], **Anna P. Petrashen**[‡], and **Arthur R. Salomon**[‡,*]

[†]Department of Molecular Pharmacology, Physiology, and Biotechnology, Brown University, Providence, Rhode Island, United States of America

[‡]Department of Molecular Biology, Cell Biology, and Biochemistry, Brown University, Providence, Rhode Island, United States of America

Abstract

Vav1, a Rac/Rho guanine nucleotide exchange factor and a critical component of the T cell receptor (TCR) signaling cascade, is rapidly tyrosine phosphorylated in response to T cell activation. Vav1 has established roles in proliferation, cytokine secretion, Ca^{2+} responses, and actin cytoskeleton regulation, however, its function in the regulation of phosphorylation of TCR components, including the ζ chain, the CD3 δ, ε, γ chains, and the associated kinases Lck, and ZAP-70 is not well established. To obtain a more comprehensive picture of the role of Vav1 in receptor proximal signaling, we performed a wide-scale characterization of Vav1-dependent tyrosine phosphorylation events using quantitative phosphoproteomic analysis of Vav1-deficient T cells across a time course of TCR stimulation. Importantly, this study revealed a new function for Vav1 in the negative feedback regulation of the phosphorylation of immunoreceptor tyrosine-based activation motifs within the ζ chains, CD3 δ, ε, γ chains, as well as activation sites on the critical T cell tyrosine kinases Itk, Lck, and ZAP-70. Our study also uncovered a previously unappreciated role for Vav1 in crosstalk between the CD28 and TCR signaling pathways.

Keywords

Phosphoproteomics; T cell receptor signaling; mass spectrometry; Vav1

Introduction

Engagement of the TCR by a cognate peptide-major histocompatibility complex (MHC) molecule activates intricate signaling cascades involving multiple enzymes, adaptors, and other cellular proteins that result in T cell activation. The Src tyrosine kinases Lck and Fyn are the first molecules recruited to the activated TCR complex, where they phosphorylate the immunoreceptor tyrosine-based activation motifs (ITAMs) of the ζ and CD3 chains (1).

To whom correspondence should be addressed: Dr. Arthur R. Salomon, art@drsalomon.com, Tel: (401) 863-6091, Fax: (401) 863-6087.

Author Contributions

The manuscript was written through contributions of all authors. All authors have given approval to the final version of the manuscript.

Phosphorylation of ITAMs leads to recruitment of the Syk family tyrosine kinase ζ-chain-associated protein kinase 70 (ZAP-70) via its tandem Src homology 2 (SH2) domains (2, 3). Subsequent activation of ZAP-70 facilitates phosphorylation of downstream adaptor proteins, resulting in the formation of a signalosome complex nucleated by linker for activation of T cells (LAT) and SH2 domain-containing leukocyte phosphoprotein of 76 kDa (SLP-76) (4, 5). This signalosome recruits a variety of effector proteins, which in turn activate a number of signaling pathways, including Ca^{2+} mobilization, activation of mitogen-activated protein kinase (MAPK) cascades, activation of transcription factors, and cytoskeletal reorganization (6, 7).

Vav1 is a member of the Dbl family of guanine nucleotide exchange factors (GEFs) exclusively expressed in hematopoietic cells (8). In T cells, Vav1 is rapidly tyrosine phosphorylated upon TCR stimulation, which activates its GEF activity towards Rac and Rho and initiates various pathways downstream of these GTPases (9–14). In addition to its function as a GEF, Vav1 has been implicated in GEF-independent roles, which is evidenced by its complex domain structure. In addition to the Dbl homology (DH) domain, which confers GEF activity, Vav1 contains a calponin homology (CH) domain, an acidic motif, a pleckstrin homology (PH) domain, a cysteine-rich domain (CRD), and a SH3-SH2-SH3 domain (15). Vav proteins are the only known Rho GEFs that combine in the same protein the DH and PH motifs, as well as the structural hallmark of signal transducer proteins, the SH2 and Src homology 3 (SH3) domains (16), suggesting that Vav1 can interact with multiple components of signal transduction pathways.

The functional importance of Vav1 has been demonstrated in thymocyte development and mature T cell activation. Mice deficient in Vav1 have a partial block at the pre-TCR checkpoint in the thymus and T cell development is strongly blocked in both positive and negative T cell selection (17–20). In mature T cells, Vav1 deficiency reduces TCR-induced proliferation, intracellular Ca^{2+} flux, upregulation of activation markers, and cytokine secretion (18, 20–25). Vav1 is also required to transduce TCR signals that lead to actin polymerization and TCR clustering (21, 25). Consistent with a role for linking TCR signaling to the actin cytoskeleton, the TCR-induced recruitment of the actin cytoskeleton to ζ chain ITAMs is impaired in Vav1-deficient T cells (21). Vav1 is also thought to play a role in the early molecular mechanisms that synergize TCR and CD28 mediating signaling (26). Interestingly, there have been contradictory observations on whether Vav1 regulates the activation of the ERK and JNK MAPKs, which requires further investigation (21, 24, 25, 27)

Although great progress has been made in understanding the role of Vav1 in TCR signaling, our understanding of the molecular mechanisms by which Vav1 regulates TCR signaling pathways downstream of TCR triggering is far from complete. The current paradigm for the role of Vav1 in TCR signaling has been developed primarily through studies investigating whether specific TCR effector functions are altered in Vav1-deficient T cells (21, 23–25, 27–31). Although these studies have been invaluable to the understanding of Vav1's role in TCR signaling, they provide little insight into the specific biochemical events that are regulated by Vav1 upstream of effector responses. Protein phosphorylation constitutes a critical mechanism for signal transduction in TCR signaling. Previous investigations of

Vav1-dependent phosphorylation events downstream of the TCR have relied solely on phosphospecific antibodies against individual, site-specific phosphorylation events or site-directed mutagenesis (21, 25, 27, 29, 31). Signal transduction networks are highly complex, and targeted interrogations of a single node provide only a narrow portal through which to view the dynamic system.

Given the critical role of Vav1 in mediating TCR signaling events, such as TCR clustering and Ca^{2+} flux, we hypothesized that this Rac/Rho GEF plays a key role in regulating tyrosine phosphorylation signaling events induced by TCR engagement. As such, MS-based quantitative phosphoproteomics was employed to gain an unbiased and wide-scale view of the role of Vav1 in TCR signaling. Thorough statistical analysis of phosphopeptide abundance changes between J.Vav1 and J.Vav1.WT cells revealed previously uncharacterized pathways regulated by Vav1, including negative feedback regulation of TCR proximal signaling. Furthermore, this phosphoproteomics approach drove the discovery of a novel function for Vav1 in regulating crosstalk between the TCR and CD28.

Experimental Methods

Cell culture, stimulation, and lysis

The J.Vav1 and J.Vav1.WT (15–11) cell lines were generously provided by Arthur Weiss (University of California San Francisco) and have been described elsewhere (27). Both cell lines were maintained in RPMI 1640 medium (Gibco, Carlsbad, CA) supplemented with 10% heat-inactivated, undialyzed FBS (HyClone, Logan, UT), 2 mM L-glutamine, 100 U/ml penicillin G, and 100 μg/ml streptomycin (Invitrogen, Carlsbad, CA) in a humidified incubator with 5% CO2 at 37°C. The J.Vav1.WT cell line medium additionally contained 0.5mg/ml Geneticin (Thermo Fisher Scientific, Rockford, IL). TCR stimulation and lysis was performed as described (32). Briefly, cells were reconstituted at a concentration of 1×10^8 cells/ml in PBS. For each stimulation time point, 1×10^8 cells were treated with OKT3 and OKT4 antibodies (eBioscience, San Diego, CA) at a concentration of 2.5 μg/ml of each antibody for 30 seconds at 37°C. Cells were then cross-linked with 22 μg/ml of goat anti-mouse IgG (Jackson ImmunoResearch, West Grove, PA) and incubated at 37°C for 0, 3, 5, or 10 minutes. In total, 5 biological replicates were performed with cells stimulated separately.

Protein reduction, alkylation, digestion, and peptide immunoprecipitation

Protein concentrations were measured using the BCA Protein Assay (Thermo Fisher Scientific). Reduction, alkylation, and trypsin digestion were performed as previously described (32). For phosphotyrosine peptide enrichment, peptide immunoprecipitation was performed using p-Tyr-100 phosphotyrosine antibody beads (Cell Signaling Technology) as previously described (32). Prior to immunoprecipitation, a 5 pmol fraction of synthetic phosphopeptide LIEDAEpYTAK was added to each individual replicate and time point sample as a normalization standard to correct for any variation in mass spectrometer sensitivity between individual replicates. Samples were then desalted using ZipTip pipette tips (EMD Millipore, Billerica, MA) according to the manufacturer's instructions.

Automated nano-LC/MS

A fully automated phosphoproteomic technology platform was implemented to quantitate tyrosine phosphopeptides as previously described (33, 34). Tyrosine phosphopeptides were analyzed by a LTQ Orbitrap Velos mass spectrometer (Thermo Fisher Scientific). Peptides were eluted through a PicoFrit analytical column (360 μm outer diameter 75 μm inner diameter-fused silica with 12 cm of 3-μm Monitor C18 particles; New Objective, Woburn, MA) with a reversed-phase gradient (0–70% 0.1M acetic acid in acetonitrile in 90 minutes). An electrospray voltage of 1.8 kV was applied using a split flow configuration, as described previously (35). Spectra were collected in positive ion mode and in cycles of one full MS scan in the Orbitrap (m/z: 300–1700), followed by data-dependent MS/MS scans in the LTQ (∼ 0.3 seconds each), sequentially of the ten most abundant ions in each MS scan with charge state screening for +1, +2, +3 ions and dynamic exclusion time of 30 seconds. The automatic gain control was 1,000,000 for the Orbitrap scan and 10,000 for the LTQ scans. The maximum ion time was 100 milliseconds for the LTQ scan and 500 milliseconds for the Orbitrap full scan. Orbitrap resolution was set at 60,000.

Database analysis

MS/MS spectra were searched against the non-redundant human UNIPROT "complete proteome set" database (UNIPROT database released 2011.10.21) containing 88,832 forward and an equivalent number of reversed decoy entries using the Mascot algorithm version 2.2.07 from Matrix Science. Peak lists were generated using extract_msn.exe (1/10/11) using a mass range of 600–4500. The Mascot database search was performed with the following parameters: trypsin enzyme specificity, 2 possible missed cleavages, 7 ppm mass tolerance for precursor ions, and 0.5 Da mass tolerance for fragment ions. Search parameters specified a differential modification of phosphorylation (+79.9663 Da) on serine, threonine, and tyrosine residues and methionine oxidation (+15.9949 Da) as well as a static modification of carbamidomethylation (+57.0215 Da) on cysteine. Mascot results were filtered by Mowse score (>20) and precursor mass error (<2ppm). Peptide assignments from the database search was filtered down to 1% FDR by a logistic spectral score, as previously described (36). The Ascore algorithm (37) was implemented to validate phosphorylation site position and the top-ranked Ascore predicted phosphorylation site position is reported (Table S1).

Relative quantitation of phosphopeptide abundance

Relative quantification of phosphopeptide abundance was performed through calculation of selected ion chromatogram (SIC) peak areas. Retention time alignment of individual replicate analyses was performed as described previously (38). Peak areas were calculated by inspection of SICs using in-house software programmed in Microsoft Visual Basic 6.0 based on Xcalibur Development kit 2.1 (Thermo Fisher Scientific). This approach used the ICIS algorithm available in the Xcalibur XDK with the following parameters: multiple resolutions of 8, noise tolerance of 0.1, noise window of 40, scans in baseline of 5, and inclusion of refexc peaks parameter value, which is false. SIC peak areas were determined for every phosphopeptide that was identified by MS/MS (34). In the case of a missing MS/MS for a particular peptide, in a particular replicate or time point, SIC peak areas were

calculated according to the peptide's isolated mass and the retention time calculated from retention time alignment. A minimum SIC peak area equivalent to the typical spectral noise level of 1000 was required of all data reported for label-free quantitation. Individual SIC peak areas were normalized to the exogenously spiked phosphopeptide LIEDAEpYTAK peak area added in the same amount to each time point and replicate sample and accompanying cellular phosphopeptides through phosphotyrosine peptide enrichment and reversed-phase elution into the mass spectrometer.

Temporal heatmaps were generated as previously described (39). The heatmap colors were generated from the average of the standard phosphopeptide normalized SICs from five biological replicate experiments. P values were calculated for each time point compared to the time point with the minimal average peak area for that phosphopeptide. A q value is defined as the measure of the minimum FDR at which a test can be called significant (40). For each time point, q values for multiple hypothesis tests were calculated based on the determined unpaired p values using the R package QVALUE as previously described (41, 42). A white dot on a label free heatmap square indicated that a significant difference (q value < 0.05; >1.5-fold or <0.67-fold) was detected for that phosphopeptide and time point relative to the time point with the minimal value (Figure S1). All of the identified peptides from each LCMS run are described in detail in Table S1 and label free quantitative data is also provided in table format in Table S2.

In a second type of heatmap, ratios from the average of 5 biological replicate experiments were generated corresponding to phosphopeptide abundance differences between J.Vav1 and J.Vav1.WT cells across the time course of receptor stimulation. For a given phosphopeptide, a black color represented a ratio of 1 between the two cell types at that time point. A red color represented less abundance, and green represented higher abundance of the given phosphopeptide in J.Vav1 cells compared to J.Vav1.WT cells. The magnitude of change of the heatmap color was calculated as described (39). Q values were also calculated based on the determined unpaired p values for each ratio heatmap square to assess the statistical significance of phosphopeptide abundance changes between J.Vav1 and J.Vav1.WT measurements for each time point across the 5 biological replicates. A white dot on a ratio heatmap square indicated that a significant difference (q value < 0.05; >1.5-fold or <0.67-fold) was detected between J.Vav1 and J.Vav1.WT measurements. All of the label-free quantitative data including calculated ratios and q values is also provided in table format in Table S2. The mass spectrometry proteomics raw data (mzXML format) and assigned MSMS spectra (pepXML) for all peptides have been deposited to the ProteomeXchange (http://proteomecentral.proteomexchange.org) via the PRIDE partner repository (43) with the dataset identifier PXD002022.

Western blotting

Immunoblots were performed as previously described using the Odyssey CLx Imaging System (Li-Cor, Lincoln, NE) (32). The following primary antibodies were from Cell Signaling Technologies: anti-GAPDH, anti-Vav1, and anti-COX IV. The anti-CD28 antibody was purchased from R&D Systems (Minneapolis, MN).

Colocalization studies

J.Vav1 and J.Vav1.WT cells were collected, washed in PBS and stimulated (where applicable) as described above. Stimulation was stopped by fixation. Both stimulated and unstimulated cells were fixed by addition of formaldehyde to a 4% concentration for 20 minutes at room temperature. Cells were permeabilized by resuspension in 2% Triton-X in PBS for 20 minutes at room temperature. Cells were then resuspended in PBS and added to coverslips previously coated in poly-L-lysine (0.01% solution, Sigma). Cells were allowed to bind for 1 hour at room temperature. Excess cell suspension was aspirated. Bound cells were washed with PBS and blocked in 1% BSA in PBS overnight at 4°C. Primary antibodies were added at 1:200 for CD3ζ (clone 6B10.2, Santa Cruz Biotechnology, Santa Cruz, CA) and 1:20 for CD28 (R&D Systems) and incubated for 3 hours. Coverslips were washed and secondary antibodies (Alexa Fluor 488 donkey anti-mouse and Alexa Fluor 647 donkey anti-goat; Abcam, Cambridge, MA) were added at 1:800 for 30 min at room temperature in the dark. Wash steps were repeated and the coverslips were mounted onto slides using Fluoromount G (Southern Biotechnology Associates, Birmingham, AL) and imaged on the Zeiss LSM710 confocal laser scanning microscope with a 63x oil magnification. Colocalization was determined using the ZEN software in which colocalization coefficients, derived from the Pearson's correlation coefficient, were calculated. Calculations were performed on 75 cells for each cell type and stimulation condition. Statistical significance was determined using Student t-tests.

Results

Label-free quantitation of TCR phosphorylation signaling events dependent on Vav1

Despite the characterization of several important pathways that are regulated by Vav1 downstream of TCR activation, our understanding of Vav1's role in mediating the critical phosphorylation cascades triggered by TCR engagement is far from complete. To determine phosphorylation pathways regulated by Vav1, a Vav1-deficient Jurkat T cell line was utilized. Traditionally, Jurkat T cell mutant cell lines have been generated using genome-wide mutagenesis (44). In this investigation, the Vav1-deficient Jurkat T cell line (J.Vav1) utilized was generated using somatic cell gene-targeting technology, which circumvents many of the disadvantages of random mutagenesis including the possibility that the selected cells have multiple fixed mutations in their genomes (27). Immunoblots confirmed Vav1 deficiency in J.Vav1 cells (Figure 1A). J.Vav1 cells with reconstituted Vav1 expression were utilized as an isogenic control, and importantly, these cells expressed levels of Vav1 levels comparable to parental Jurkat T cells (Figure 1B).

In this study, a phosphoproteomic investigation of Vav1-deficient (J.Vav1) and Vav1-reconstituted (J.Vav1.WT) Jurkat T cells across four time points of TCR stimulation was performed to elucidate the role of Vav1 in TCR signaling. The four time point selected for study have been previously shown to encompass peak tyrosine phosphorylation reached at 3 minutes, as well as decreased phosphorylation at 5 minutes, with tyrosine phosphorylation reaching basal levels at 10 minutes (32, 39, 45). For each cell type and time point, a total of 5 biological replicates were analyzed using a LC-MS/MS approach (Figure 2). The complete list of quantitative data from every unique sequence and phosphorylation site identified by

MSMS database search at 1% FDR in each replicate and time point is included in Supplemental Information (Table S2). In addition, the annotated MSMS spectra for all phosphopeptides from this study and a complete list of tyrosine phosphorylated peptides with MOWSE score >20 including reversed database hits from every replicate and time point of TCR stimulation are found in the supplement (Figure S2, Table S1). Data are also available via ProteomeXchange with identifier PXD002022 (Username reviewer39846@ebi.ac.uk and Password is qH7oHpsp). The analysis of pairwise replicate SIC peak area correlation indicated the high degree of quantitative reproducibility between individual LC/MS runs used for label free intensity-based quantitation (average R value of 0.84 +/− 0.03; Figure S3). A total of 692 unique tyrosine phosphopeptides containing 652 unique tyrosine phosphorylation sites on 438 proteins were identified at a 1% false discovery rate (FDR).

To visualize the phosphoproteomic data, two types of heatmaps were generated. Temporal heatmaps visualize phosphorylation dynamics in one cell type across TCR stimulation, and ratio heatmaps represent phosphorylation changes between J.Vav1 and J.Vav1.WT cells for each time point. Stringent statistical tests were performed on the peak areas of confidently assigned phosphopeptides to ascertain biologically relevant conclusions as described in Experimental Procedures. The detection of significantly altered phosphopeptides was carried out applying student's t test to the five biological replicate peak areas corrected for multiple hypotheses by q value. A volcano plot representing the relationship between fold change and q value illustrates statistically significant observations (Figure S1). Statistical significance was conservatively attributed to quantified phosphopeptides with q values less than 0.05, and fold change <0.67 or >1.5, represented as white dots within individual heatmap squares. Discussions and conclusions are exclusively drawn from statistically significant observations using these specific criteria.

A hallmark of T cell activation is the induction of tyrosine phosphorylation cascades downstream of the TCR. Histogram representations from J.Vav1.WT samples show overall increases in phosphopeptide peak areas from 0 to 3 minutes of TCR stimulation that return to basal levels at 5 and 10 minutes (Figure S4). This pattern is also observed in phosphopeptide peak areas from the KEGG TCR signaling pathway (Figure S4). Furthermore, temporal heatmaps representing phosphorylation dynamics on previously characterized tyrosine sites across the time course of TCR stimulation were generated for J.Vav1.WT cells (Figure S5). Phosphorylation of TCR proximal proteins followed expected patterns, with statistically significant increases in phosphorylation from 0 to 3 minutes of TCR stimulation that tapered off between 5 and 10 minutes.

Vav1 regulates a negative feedback pathway in TCR signaling

To visualize the global effects of Vav1 deficiency on the canonical TCR signaling pathway, ratio heatmaps were generated for phosphosites on proteins that had at least one statistically significant (q value < 0.05; >1.5-fold or <0.67-fold change) heatmap square (Figure 3). Surprisingly, the majority of identified tyrosine sites on TCR proximal signaling proteins had statistically significant elevated phosphorylation in Vav1-deficient cells relative to controls. This observation was corroborated in a histogram representation of J.Vav1 to

J.Vav1.WT ratios across the four time points of TCR stimulation (Figure S6). In particular, we observed statistically significant (q value < 0.05; >1.5-fold or <0.67-fold) elevated phosphorylation on Tyr^{394}, the positive regulatory site of the Src kinase Lck, across all time points of TCR stimulation. We also observed statistically significant (q value < 0.05; >1.5-fold or <0.67-fold) elevated phosphorylation on the negative regulatory site of Lck, Tyr^{505}, at 5 and 10 minutes of TCR stimulation. The implication of this finding is elaborated in the Discussion. This pattern of statistically significant elevated phosphorylation was observed on the majority of ζ chain and CD3 chain ITAMs in response to Vav1 deficiency, well-defined substrates of Lck kinase activity. The Src family kinase Fyn also had altered phosphorylation in J.Vav1 cells, although the functions of the identified sites are currently unknown. These observations point to a previously unappreciated role for Vav1 in the negative regulation of Lck kinase activity and receptor phosphorylation.

Sites on another critical TCR proximal kinase, ZAP-70, also had statistically significant (q value < 0.05; >1.5-fold or <0.67-fold) elevated phosphorylation in Vav1-deficient cells. For example, we observed statistically significant elevated phosphorylation on Tyr^{492}Tyr^{493} at 10 minutes and Tyr^{292} at 3, 5, and 10 minutes of TCR stimulation, substrates of Lck kinase activity. Additionally, Tyr^{397} showed statistically significant decreased phosphorylation at 5 minutes of TCR stimulation, a site thought to stabilize the inactive conformation of ZAP-70 (46). These observations suggest that Vav1 plays a previously unappreciated role in the regulation of ZAP-70 phosphorylation and are further elaborated in the Discussion.

A number of well-established receptor proximal negative regulators of TCR signaling had statistically significant (q value < 0.05; >1.5-fold or <0.67-fold) elevated phosphorylation in Vav1-deficient T cells, including PAG, Cbl-b, CD5, CD31, SIT and SHP-1. Importantly, a number of these sites are established substrates of Lck catalytic activity, including Tyr^{453} of CD5 (47, 48), as well as Tyr^{536} and Tyr^{564} of SHP-1 (49), further substantiating the presence of elevated Lck kinase activity in Vav1-deficient T cells.

Downstream of the TCR, we observed statistically significant (q value < 0.05; >1.5-fold or <0.67-fold) alterations in phosphorylation on proteins associated with the signalosome complex nucleated by SLP-76 and LAT, including ADAP, Itk, and SHC1. The N-terminal phosphorylation sites on SLP-76, Tyr^{113} and Tyr^{128}, which are critical for SLP-76 function (50, 51), are located within a large (greater than 30 amino acid) tryptic peptide and thus were not detected in this investigation. On the Tec kinase Itk, we observed statistically significant increases in phosphorylation on its positive regulatory site Tyr^{512} at 5 and 10 minutes of TCR stimulation, a substrate of Lck (52). SHC1 also had greater than 8.5-fold statistically significant elevated phosphorylation on Tyr^{427} at 5 and 10 minutes of TCR stimulation, a site that recruits Grb2 and SOS to the plasma membrane and promotes ERK activation (53, 54). In line with these observations, we observed statistically significant elevated phosphorylation on the positive regulatory sites of ERK at 5 and 10 minutes of TCR stimulation in Vav1-deficient cells. This pattern was also identified on positive regulatory sites of the MAPKs JNK1/2, and p38α/γ at 5 and 10 minutes of TCR stimulation in the phosphoproteomic data.

Vav1 regulates phosphorylation of CD28 and PI3K

Upon TCR stimulation, CD28 phosphorylation at Tyr^{191} provides a docking site for the SH2 domains of the p85 subunit of phosphoinositide 3-kinase (PI3K), Grb2 and GADS (55, 56). In Vav1-deficient cells, phosphorylation of Tyr^{191} was elevated at 5 minutes of TCR stimulation relative to controls. Conversely, statistically significant (q value < 0.05; >1.5-fold or <0.67-fold) decreases in CD28 phosphorylation on Tyr^{206}Tyr^{209} and Tyr^{218} were observed (Figure 4A). These three sites have been shown to mediate CD69 expression and IL-2 secretion (57, 58). Western blot analysis of CD28 expression confirmed that observed differences in phosphorylation were not a function of altered protein expression levels in J.Vav1 cells (Figure 4B). The altered phosphorylation on CD28 observed in Vav1-deficient T cells suggests Vav1 regulates crosstalk between the TCR and CD28. Downstream of CD28, statistically significant decreases in tyrosine phosphorylation were observed on the regulatory subunit of PI3K, including Tyr^{464} of p85β and Tyr^{467}of p85α. Conversely, Tyr^{580} of p85a had statistically significant elevated phosphorylation at 5 and 10 minutes of TCR stimulation. The phosphorylation of Tyr^{467} on p85α has been reported to track with the activation of this kinase (59–61), suggesting reduced activity of PI3K in Vav1-deficient cells.

Vav1 mediates colocalization of CD28 and ζ chain in TCR-stimulated cells

It has been previously established that Itk, as well as Lck, phosphorylate the C-terminal tyrosine sites on CD28 in Jurkat T cells (62). Despite the observed elevated phosphorylation on both the positive regulatory sites of both these kinases as well as their known substrates in J.Vav1 cells, constitutive decreases in phosphorylation were identified on their putative CD28 tyrosine site substrates. We hypothesized that Vav1 may play an important scaffolding function for CD28 by recruiting it to the proximity of the TCR for phosphorylation in the absence of CD28 costimulation. To investigate the role of Vav1 in TCR-mediated CD28 phosphorylation, colocalization studies were performed to assess the proximity of CD28 to the ζ chain of the TCR as both kinases are enriched in membrane complexes with the TCR (63) (Figure 5A). A statistically significant (p value < 0.00001) decrease in the degree of colocalization between CD28 and the ζ chain was observed in J.Vav1 cells stimulated for 3 minutes (Figure 5B). The combination of the proteomic data and colocalization data support the model that Vav1 plays an unappreciated role in the recruitment of CD28 to the TCR in CD3/CD4-crosslinked cells leading to reduction in PI3K activity in the absence of CD28 costimulation.

Discussion

Protein phosphorylation constitutes a critical mechanism for signaling events downstream of the TCR. The MS-based phosphoproteomic approach used in this study provides detailed quantitative information on tyrosine phosphorylation of specific sites, allowing for the discrimination between their different roles. Importantly, a previously unobserved negative feedback pathway regulated by Vav1 was identified in this phosphoproteomic investigation. Furthermore, the phosphoproteomic approach utilized drove the discovery of a previously unappreciated role for Vav1 in mediating CD28 localization to the TCR and activation of PI3K in CD3/CD4 crosslinked cells.

Previous studies investigating the role of Vav1 have reported no effect of Vav1 deficiency on the phosphorylation of upstream TCR signaling proteins, including ZAP-70, Lck, and the CD3 chains, as well as downstream ERK (23, 25, 31, 64). It cannot be ruled out that the discrepancies in observations made in this investigation with other studies are a consequence of the cell type and stimulation method used. Indeed, stimulation of the TCR pathway using soluble anti-CD3/CD4 antibodies may generate different phosphoproteomic profiles from T cells stimulated by immobilized antibody or by APCs presenting agonist peptide. However, many of the methods used to determine these findings relied on the use of pan-specific anti-phosphotyrosine antibodies against targeted immunoprecipitated proteins in Western blots. The combined average abundance of phosphorylation on numerous tyrosine residues is measured by these other approaches, and information about individual phosphorylation sites are not revealed. A MS-based approach that quantitates peak areas of individual phosphopeptides provides accurate and robust quantification of phosphorylation changes.

One striking finding made in this phosphoproteomic investigation was the elevated phosphorylation of key regulators of TCR signaling in Vav1-deficient cells, revealing a negative feedback loop regulated by Vav1. Interestingly, Lck, a critical driver of TCR signaling, had elevated phosphorylation on both its positive and negative regulatory sites in J.Vav1 cells. A previous study has demonstrated that dephosphorylation of Tyr^{505}, the negative regulatory site of Lck, is not a prerequisite for phosphorylation of Lck at Tyr^{394} or activation of the kinase, and that Lck is catalytically active when it is phosphorylated on both Tyr^{394} and Tyr^{505} (65). Moreover, at these time points, statistically significant elevated phosphorylation of a large number of previously established Lck substrates was observed, including Tyr^{453} of CD5, the ζ and CD3 chain ITAMs, Tyr^{427} of SHC1, and Tyr^{512} of Itk. These phosphoproteomic observations indicate that Vav1 deficiency elevates both the phosphorylation status and catalytic activity of Lck in our system. Further downstream in this pathway, elevated phosphorylation on the positive regulatory sites of ERK at 5 and 10 minutes of TCR stimulation was observed in phosphoproteomic experiments, suggesting the elevated activity of this kinase. Additionally, the other major stress kinases JNK1/2 and p38 also showed elevated phosphorylation on their positive regulatory sites at 5 and 10 minutes of TCR stimulation. The increased phosphorylation of these sites corresponds to that of upstream Tyr^{427} on SHC1, a mediator of activation of these kinases, as well as a substrate of Lck activity (53, 54). From this data, a previously unappreciated link between Vav1 expression and Lck kinase activity has been uncovered.

Interestingly, the pattern of elevated phosphorylation on positive regulators of TCR signaling observed in Vav1-deficient T cells was coupled with elevated phosphorylation on negative regulators of TCR signaling. For example, phosphorylation of Tyr^{292} on ZAP-70 was elevated in J.Vav1 cells. Previous work has demonstrated hyperphosphorylation of LAT and SLP-76 in Y292F mutant T cells (66). Other negative regulators identified in this dataset mediate their negative feedback on TCR signaling via modification of tyrosine phosphorylation on Lck itself. For example, we observed elevated phosphorylation of PAG in Vav1-deficient cells. In unstimulated cells, PAG is tyrosine phosphorylated and associated with Csk, a cytoplasmic protein tyrosine kinase responsible for inhibition of Lck by phosphorylating its inhibitory tyrosine (Tyr^{505}) (67). Observed elevated phosphorylation on Tyr^{317} of PAG, the recruitment site of Csk to PAG, suggests Csk proximity to Lck and

may account for the observed elevated phosphorylation on Tyr^{505} of Lck. SHP-1 regulates Lck kinase activity through dephosphorylation of Tyr^{394} and is essential for termination of TCR signaling. Phosphorylation of SHP-1 was elevated on Tyr^{536} and Tyr^{564} in Vav1-deficient cells at 5 and 10 minutes of TCR signaling, sites that increases its phosphatase activity (49). Despite elevated phosphorylation of SHP-1, and thus elevated phosphatase activity, decreases in its tyrosine phosphorylation site substrates, including Y^{394} of Lck and Y^{713} of CD31, were not observed. One potential mechanism that may be at play is ERK feedback to Lck, in which phosphorylation of Ser^{59} of Lck by ERK protects Lck from dephosphorylation by SHP-1 (68). These observations reveal that elevated phosphorylation of negative regulators of TCR signaling does not dampen wide-scale phosphorylation of positive regulators in TCR-stimulated Vav1-deficient cells.

The mechanism by which Vav1 deficiency accounts for the observed elevation of phosphorylation on Lck, its downstream targets, as well as on negative regulators of TCR signaling is unknown. A critical component of TCR signaling involves the formation of microclusters, which concentrate the upstream TCR signaling proteins that propagate signaling pathways to downstream pathways (69). Vav1 rapidly assembles into TCR-induced microclusters (70) and Vav1-deficient cells have defective TCR microcluster formation upon TCR stimulation (25). Furthermore, Vav1 stabilizes the complex protein-protein interactions that associate around the LAT-SLP-76 complex (71, 72). For example, Vav1 has been shown to positively regulate the TCR-induced association between PLCγ1 and SLP-76 (29). In addition, the SH2 and SH3 domains of Vav1 have been shown to interact with Shc, SLP-76, NCK, SLP-76, ZAP-70, Grb2, and Crk (73–77). Vav1 deficiency may alter the arrangement and/or localization of these various proteins, resulting in the elevated phosphorylation observed in this investigation.

The elevated phosphorylation observed in Vav1-deficient cells may also be a consequence of decreased activity and/or localization of a phosphatase. SHP1 is thought to play a critical role in the termination of TCR signaling acting, at least in part, through the dephosphorylation and inactivation of Src family kinases (78). Although the precise molecular mechanisms of SHP-1 recruitment into the TCR/CD3 complex are unclear, several potential binding partners for SHP-1 have been proposed, including Vav1 (79). Indeed, co-immunoprecipitation experiments in EL4 cell lines and murine splenic cells have demonstrated an association between SHP-1 and Vav1 that is markedly increased in response to mitogenic stimulation. Furthermore, Vav1 immunoprecipitates from these cells had phosphatase activity and a substantial portion of total cellular SHP-1 activity was associated with Vav1 (79). In a study by Pani et al., a number of Vav1-associated proteins in SHP-1-deficient T cells were shown to be hyperphosphorylated in response to TCR ligation, suggesting that Vav1 positions SHP-1 to facilitate dephosphorylation of T cell signaling components (80). In another investigation, a trapping mutation was introduced into the catalytic site of SHP-1 in order to isolate SHP-1 substrates in NK cells. Intriguingly, Vav1 was the only protein detectably associated with the catalytic site of SHP-1 in this system (81). Thus, given the elevated phosphorylation on a number of critical tyrosine sites proximal to the TCR in Vav1-deficient cells presented in this phosphoproteomic investigation, along with previous findings linking SHP-1 to Vav1, we propose a model in which Vav1 recruits SHP-1 to regulate Lck activity leading to altered phosphorylation of

CD3 and ζ ITAMs, as well as ZAP-70 in TCR stimulated cells (Figure 6A). Alternatively, Vav1 recruitment of SHP-1 to the TCR could directly regulate ITAM and ZAP-70 phosphorylation.

Jurkat T cells are deficient in the lipid phosphatases PTEN and SHIP, which complicates the study of pathways downstream of PI3K in these cells and the new functions attributed to Vav1 revealed in this manuscript should be studied in primary T cells in the future. For this reason, we focused on tyrosine phosphorylation events upstream of pathways regulated by lipid phosphatase products (i.e. CD28 and PI3K). In this dataset, statistically significant decreases in phosphorylation on $Tyr^{206}Tyr^{209}$ and Tyr^{218} of CD28 were observed in CD3/CD4 crosslinked cells as a result of Vav1 deficiency. CD3 stimulation alone has been shown to mediate the phosphorylation of CD28 distal sites in wild type Jurkat T cells (32, 82), suggesting crosstalk between these two critical receptors. Critically, Tyr^{209} has been demonstrated to be both necessary and sufficient for CD69 expression and IL-2 induction (57). Itk has been shown to phosphorylate all four distal tyrosines of CD28 in Jurkat T cells (62). Because both Itk and Lck kinase activity appeared to be elevated as a result of Vav1 deficiency, it was hypothesized that the defect in CD28 phosphorylation was due to a defect in the localization of CD28 to the vicinity of these kinases. Confocal microscopy confirmed that Vav1 deficiency resulted in reduced colocalization of CD28 to the ζ chain upon TCR stimulation. Thus, using a phosphoproteomic approach, we were able to identify a novel mechanism in which Vav1 mediates the proximity of CD28 to the TCR and its subsequent phosphorylation.

Various hypotheses can be made regarding the mechanism by which Vav1 regulates CD28 localization to the TCR. CD28 has a highly conserved and relatively short cytoplasmic tail that has several motifs important for its function, including: four tyrosine residues, four serine residues, two threonine residues, two PxxP motifs, and two lysine residues (83). Phosphorylation of the tyrosine sites provides docking sites for SH2 domain containing proteins whereas the proline-rich motifs can bind SH3 domain containing proteins. Previous work has shown that Vav1 can associate with CD28 via its association with Grb2 or GADS, which can bind to either the tyrosine sites or PxxP motifs via their SH2 or SH3 domains, respectively (9, 84–87). Our data supports a model where Vav1 recruits Lck and/or Itk to CD28 through Grb2 and/or GADS (Figure 6B). Our data also supports a model of Vav1-mediated recruitment of CD28 to the TCR through regulation of the actin cytoskeleton. As previously noted, Vav1-deficient cells have defects in cortical actin cytoskeleton changes in TCR signaling (21, 25, 28, 30, 70, 88, 89). The PYAP motif of CD28 (which contains Tyr^{209}) has been shown to bind with filamin-A, which tethers CD28 to lipid rafts and recruits Rac/Rho GTPases to the vicinity of Vav1 in T cells. Importantly, CD28 ligation results in the co-immunoprecipitation of Vav1 and filamin-A with CD28 in Jurkat T cells (90). Altogether, this model proposes that Vav1 deficiency results in defective Rac/Rho GTPase activation leading to defects in cytoskeletal rearrangements required for CD28 localization to the TCR (Figure 6B).

In this dataset, decreases in phosphorylation on Tyr^{464} and Tyr^{467} of PI3K p85 were observed. Defective activation of PI3K has been reported in Vav1-deficient DP thymocytes through observations of decreased TCR-induced Akt phosphorylation (29). Furthermore,

tyrosine phosphorylation of the p85 subunit has been shown to be a requirement for induction of the lipid kinase activity of the p110 subunit (91), suggesting that PI3K activity is decreased in T cell lacking Vav1. The observed reduction in PI3K phosphorylation may be a result of the defective localization of CD28 to the TCR in Vav1-deficient cells as described above, as CD28 is a critical scaffold for PI3K, and Vav1 has been shown to regulate the PI3K-Akt pathway downstream of the TCR (83). In addition, previous studies have shown that Vav1 can associate with the p85 subunit of PI3K (92, 93), which may be a critical mechanism for its activation upon TCR stimulation. Alternatively, Rac1 association with PI3K has been observed, suggesting that Vav1 may regulate PI3K through its GEF activity on Rac1 (94). Overall, the observations on PI3K corroborate previous findings of IL-2 secretion defects in Vav1-deficient T cells and suggest a potential link between Vav1 deficiency and defective IL-2 secretion.

A MS-based phosphoproteomics strategy was utilized to precisely quantify tyrosine phosphorylation dynamics in T cells lacking Vav1 expression. From the temporal and quantitative data, new biological insights have been made into the role of Vav1 in the regulation of signaling pathways downstream of the TCR. Importantly, we have identified a novel role for Vav1 in regulating negative feedback pathways to the TCR itself. Furthermore, phosphoproteomic analysis has revealed that Vav1 serves as an important link between TCR signaling and CD28 phosphorylation. These observations begin to reveal the diverse constellation of mechanisms mediated by Vav1 to maintain the proper equilibrium of T cell activation through negative feedback pathways and deepen our understanding of the intrinsic connections between TCR and CD28 co-receptor signaling pathways in the absence of co-receptor ligand binding.

Supplementary Material

Refer to Web version on PubMed Central for supplementary material.

ACKNOWLEDGMENTS

ABBREVIATIONS

BCA	bicinchoninic acid
Cbl-b	casitas B-lineage lymphoma proto-oncogene b
CH	calponin homology
CRD	cysteine-rich domain

DH	Dbl-homology
ERK1/2	extracellular signal-regulated kinase-1/2
FBS	fetal bovine serum
FDR	false discovery rate
GEF	guanine nucleotide exchange factor
ITAM	immunoreceptor tyrosine-based activation motif
Itk	IL2-inducible T-cell kinase
JE6-1	Jurkat clone E6-1
KEGG	Kyoto Encyclopedia of Genes and Genomes
LAT	linker for activation of T cells
LTQ	linear trap quadrupole
MAPK	mitogen activated protein kinase
MHC	major histocompatibility complex
PAG	phosphoprotein associated glycolipid-enriched membrane protein
PH	pleckstrin homology
PI3K	phosphoinositide 3-kinase
PLCγ1	phospholipase c gamma 1
SH2	Src homology 2
SH3	Src homology 3
SHP-1/2	SH2 domain-containing protein tyrosine phosphatase 1/2
SIC	select ion chromatogram
SLP-76	SH2 domain-containing leukocyte phosphoprotein of 76 kDa
TCR	T cell receptor
ZAP-70	ζ-chain-associated protein kinase 70

REFERENCES

1. van Oers NS, Killeen N, Weiss A. Lck regulates the tyrosine phosphorylation of the T cell receptor subunits and ZAP-70 in murine thymocytes. J Exp Med. 1996; 183(3):1053–1062. [PubMed: 8642247]

2. van Oers NS, Killeen N, Weiss A. ZAP-70 is constitutively associated with tyrosine-phosphorylated TCR zeta in murine thymocytes and lymph node T cells. Immunity. 1994; 1(8):675–685. [PubMed: 7600293]

3. Au-Yeung BB, Deindl S, Hsu LY, Palacios EH, Levin SE, Kuriyan J, Weiss A. The structure, regulation, and function of ZAP-70. Immunol Rev. 2009; 228(1):41–57. [PubMed: 19290920]

4. Zhang W, Sloan-Lancaster J, Kitchen J, Trible RP, Samelson LE. LAT: the ZAP-70 tyrosine kinase substrate that links T cell receptor to cellular activation. Cell. 1998; 92(1):83–92. [PubMed: 9489702]

5. Zhang W, Trible RP, Zhu M, Liu SK, McGlade CJ, Samelson LE. Association of Grb2, Gads, and phospholipase C-gamma 1 with phosphorylated LAT tyrosine residues. Effect of LAT tyrosine mutations on T cell angien receptor-mediated signaling. J Biol Chem. 2000; 275(30):23355–23361. [PubMed: 10811803]

6. Smith-Garvin JE, Koretzky GA, Jordan MS. T cell activation. Annu Rev Immunol. 2009; 27:591–619. [PubMed: 19132916]

7. Kane LP, Lin J, Weiss A. Signal transduction by the TCR for antigen. Curr Opin Immunol. 2000; 12(3):242–249. [PubMed: 10781399]

8. Katzav S, Martin-Zanca D, Barbacid M. vav, a novel human oncogene derived from a locus ubiquitously expressed in hematopoietic cells. EMBO J. 1989; 8(8):2283–2290. [PubMed: 2477241]

9. Bustelo XR. Regulatory and signaling properties of the Vav family. Mol Cell Biol. 2000; 20(5):1461–1477. [PubMed: 10669724]

10. Crespo P, Schuebel KE, Ostrom AA, Gutkind JS, Bustelo XR. Phosphotyrosine-dependent activation of Rac-1 GDP/GTP exchange by the vav proto-oncogene product. Nature. 1997; 385(6612):169–172. [PubMed: 8990121]

11. Han J, Das B, Wei W, Van Aelst L, Mosteller RD, Khosravi-Far R, Westwick JK, Der CJ, Broek D. Lck regulates Vav activation of members of the Rho family of GTPases. Mol Cell Biol. 1997; 17(3):1346–1353. [PubMed: 9032261]

12. Han J, Luby-Phelps K, Das B, Shu X, Xia Y, Mosteller RD, Krishna UM, Falck JR, White MA, Broek D. Role of substrates and products of PI 3-kinase in regulating activation of Rac-related guanosine triphosphatases by Vav. Science. 1998; 279(5350):558–560. [PubMed: 9438848]

13. Bustelo XR, Ledbetter JA, Barbacid M. Product of vav proto-oncogene defines a new class of tyrosine protein kinase substrates. Nature. 1992; 356(6364):68–71. [PubMed: 1311423]

14. Margolis B, Hu P, Katzav S, Li W, Oliver JM, Ullrich A, Weiss A, Schlessinger J. Tyrosine phosphorylation of vav proto-oncogene product containing SH2 domain and transcription factor motifs. Nature. 1992; 356(6364):71–74. [PubMed: 1531699]

15. Zugaza JL, Lopez-Lago MA, Caloca MJ, Dosil M, Movilla N, Bustelo XR. Structural determinants for the biological activity of Vav proteins. J Biol Chem. 2002; 277(47):45377–45392. [PubMed: 12228230]

16. Bustelo XR. Regulatory and signaling properties of the Vav family. Molecular and cellular biology. 2000; 20(5):1461–1477. [PubMed: 10669724]

17. Turner M, Mee PJ, Walters AE, Quinn ME, Mellor AL, Zamoyska R, Tybulewicz VL. A requirement for the Rho-family GTP exchange factor Vav in positive and negative selection of thymocytes. Immunity. 1997; 7(4):451–460. [PubMed: 9354466]

18. Zhang R, Alt FW, Davidson L, Orkin SH, Swat W. Defective signalling through the T- and B-cell antigen receptors in lymphoid cells lacking the vav proto-oncogene. Nature. 1995; 374(6521):470–473. [PubMed: 7700359]

19. Fischer KD, Zmuldzinas A, Gardner S, Barbacid M, Bernstein A, Guidos C. Defective T-cell receptor signalling and positive selection of Vav-deficient CD4+ CD8+ thymocytes. Nature. 1995; 374(6521):474–477. [PubMed: 7700360]

20. Tarakhovsky A, Turner M, Schaal S, Mee PJ, Duddy LP, Rajewsky K, Tybulewicz VL. Defective antigen receptor-mediated proliferation of B and T cells in the absence of Vav. Nature. 1995; 374(6521):467–470. [PubMed: 7700358]

21. Fischer KD, Kong YY, Nishina H, Tedford K, Marengere LE, Kozieradzki I, Sasaki T, Starr M, Chan G, Gardener S, Nghiem MP, Bouchard D, Barbacid M, Bernstein A, Penninger JM. Vav is a regulator of cytoskeletal reorganization mediated by the T-cell receptor. Curr Biol. 1998; 8(10):554–562. [PubMed: 9601639]

22. Penninger JM, Fischer KD, Sasaki T, Kozieradzki I, Le J, Tedford K, Bachmaier K, Ohashi PS, Bachmann MF. The oncogene product Vav is a crucial regulator of primary cytotoxic T cell responses but has no apparent role in CD28-mediated co-stimulation. Eur J Immunol. 1999; 29(5):1709–1718. [PubMed: 10359126]

23. Fischer KD, Tedford K, Penninger JM. Vav links antigen-receptor signaling to the actin cytoskeleton. Semin Immunol. 1998; 10(4):317–327. [PubMed: 9695188]

24. Costello PS, Walters AE, Mee PJ, Turner M, Reynolds LF, Prisco A, Sarner N, Zamoyska R, Tybulewicz VL. The Rho-family GTP exchange factor Vav is a critical transducer of T cell receptor signals to the calcium, ERK, and NF-kappaB pathways. Proc Natl Acad Sci USA. 1999; 96(6):3035–3040. [PubMed: 10077632]

25. Holsinger LJ, Graef IA, Swat W, Chi T, Bautista DM, Davidson L, Lewis RS, Alt FW, Crabtree GR. Defects in actin-cap formation in Vav-deficient mice implicate an actin requirement for lymphocyte signal transduction. Curr Biol. 1998; 8(10):563–572. [PubMed: 9601640]

26. Hehner SP, Hofmann TG, Dienz O, Droge W, Schmitz ML. Tyrosine-phosphorylated Vav1 as a point of integration for T-cell receptor- and CD28-mediated activation of JNK, p38, and interleukin-2 transcription. J Biol Chem. 2000; 275(24):18160–18171. [PubMed: 10849438]

27. Cao Y, Janssen EM, Duncan AW, Altman A, Billadeau DD, Abraham RT. Pleiotropic defects in TCR signaling in a Vav-1-null Jurkat T-cell line. EMBO J. 2002; 21(18):4809–4819. [PubMed: 12234921]

28. Villalba M, Bi K, Rodriguez F, Tanaka Y, Schoenberger S, Altman A. Vav1/Rac-dependent actin cytoskeleton reorganization is required for lipid raft clustering in T cells. J Cell Biol. 2001; 155(3): 331–338. [PubMed: 11684704]

29. Reynolds LF, Smyth LA, Norton T, Freshney N, Downward J, Kioussis D, Tybulewicz VL. Vav1 transduces T cell receptor signals to the activation of phospholipase C-gamma1 via phosphoinositide 3-kinase-dependent and -independent pathways. J Exp Med. 2002; 195(9):1103–1114. [PubMed: 11994416]

30. Ardouin L, Bracke M, Mathiot A, Pagakis SN, Norton T, Hogg N, Tybulewicz VL. Vav1 transduces TCR signals required for LFA-1 function and cell polarization at the immunological synapse. Eur J Immunol. 2003; 33(3):790–797. [PubMed: 12616499]

31. Reynolds LF, de Bettignies C, Norton T, Beeser A, Chernoff J, Tybulewicz VL. Vav1 transduces T cell receptor signals to the activation of the Ras/ERK pathway via LAT, Sos, and RasGRP1. J Biol Chem. 2004; 279(18):18239–18246. [PubMed: 14764585]

32. Helou YA, Nguyen V, Beik SP, Salomon AR. ERK positive feedback regulates a widespread network of tyrosine phosphorylation sites across canonical T cell signaling and actin cytoskeletal proteins in Jurkat T cells. PLoS One. 2013; 8(7):e69641. [PubMed: 23874979]

33. Yu K, Salomon AR. PeptideDepot: flexible relational database for visual analysis of quantitative proteomic data and integration of existing protein information. Proteomics. 2009; 9(23):5350–5358. [PubMed: 19834895]

34. Yu K, Salomon AR. HTAPP: high-throughput autonomous proteomic pipeline. Proteomics. 2010; 10(11):2113–2122. [PubMed: 20336676]

35. Ficarro SB, Salomon AR, Brill LM, Mason DE, Stettler-Gill M, Brock A, Peters EC. Automated immobilized metal affinity chromatography/nano-liquid chromatography/electrospray ionization mass spectrometry platform for profiling protein phosphorylation sites. Rapid Communications in Mass Spectrometry. 2005; 19(1):57–71. [PubMed: 15570572]

36. Yu K, Sabelli A, DeKeukelaere L, Park R, Sindi S, Gatsonis CA, Salomon A. Integrated platform for manual and high-throughput statistical validation of tandem mass spectra. Proteomics. 2009; 9(11):3115–3125. [PubMed: 19526561]

37. Beausoleil SA, Villen J, Gerber SA, Rush J, Gygi SP. A probability-based approach for high-throughput protein phosphorylation analysis and site localization. Nat Biotechnol. 2006; 24(10):1285–1292. [PubMed: 16964243]

38. Demirkan G, Yu K, Boylan JM, Salomon AR, Gruppuso PA. Phosphoproteomic profiling of in vivo signaling in liver by the mammalian target of rapamycin complex 1 (mTORC1). PLoS One. 2011; 6(6):e21729. [PubMed: 21738781]

39. Nguyen V, Cao L, Lin JT, Hung N, Ritz A, Yu K, Jianu R, Raphael BJ, Ulin S, Laidlaw DH, Brossay L, Salomon AR. A new approach for quantitative phosphoproteomic dissection of signaling pathways applied to T cell receptor activation. Mol Cell Proteomics. 2009 In Press.

40. Storey JD. A direct approach to false discovery rates. Journal of the Royal Statistical Society Series B-Statistical Methodology. 2002; 64:479–498.

41. Storey JD. The positive false discovery rate: A Bayesian interpretation and the q-value. Annals of Statistics. 2003; 31(6):2013–2035.

42. Storey JD, Tibshirani R. Statistical significance for genomewide studies. Proc Natl Acad Sci USA. 2003; 100(16):9440–9445. [PubMed: 12883005]

43. Vizcaino JA, Cote RG, Csordas A, Dianes JA, Fabregat A, Foster JM, Griss J, Alpi E, Birim M, Contell J, O'Kelly G, Schoenegger A, Ovelleiro D, Perez-Riverol Y, Reisinger F, Rios D, Wang R, Hermjakob H. The PRoteomics IDEntifications (PRIDE) database and associated tools: status in 2013. Nucleic Acids Research. 2013; 41:D1063–D1069. (Database issue), [PubMed: 23203882]

44. Goldsmith MA, Bockenstedt LK, Dazin P, Weiss A. Use of somatic cell mutants to study the signal transduction function of the T cell antigen receptor. Adv Exp Med Biol. 1989; 254:25–33. [PubMed: 2573246]

45. Ji Q, Ding Y, Salomon AR. SLP-76 N-terminal tyrosine residues regulate a dynamic signaling equilibrium involving feedback of proximal TCR signaling. Mol Cell Proteomics. 2014

46. Yan Q, Barros T, Visperas PR, Deindl S, Kadlecek TA, Weiss A, Kuriyan J. Structural basis for activation of ZAP-70 by phosphorylation of the SH2-kinase linker. Mol Cell Biol. 2013; 33(11): 2188–2201. [PubMed: 23530057]

47. Vila JM, Gimferrer I, Padilla O, Arman M, Places L, Simarro M, Vives J, Lozano F. Residues Y429 and Y463 of the human CD5 are targeted by protein tyrosine kinases. Eur J Immunol. 2001; 31(4):1191–1198. [PubMed: 11298344]

48. Dennehy KM, Ferris WF, Veenstra H, Zuckerman LA, Killeen N, Beyers AD. Determination of the tyrosine phosphorylation sites in the T cell transmembrane glycoprotein CD5. Int Immunol. 2001; 13(2):149–156. [PubMed: 11157848]

49. Lorenz U, Ravichandran KS, Pei D, Walsh CT, Burakoff SJ, Neel BG. Independent tyrosyl phosphorylation of the phosphotyrosine phosphatase SH-PTP1 in murine T cells. Mol Cell Biol. 1994; 14(3):1824–1834. [PubMed: 8114715]

50. Jordan MS, Smith JE, Burns JC, Austin JE, Nichols KE, Aschenbrenner AC, Koretzky GA. Complementation in trans of altered thymocyte development in mice expressing mutant forms of the adaptor molecule SLP76. Immunity. 2008; 28(3):359–369. [PubMed: 18342008]

51. Bubeck Wardenburg J, Fu C, Jackman JK, Flotow H, Wilkinson SE, Williams DH, Johnson R, Kong G, Chan AC, Findell PR. Phosphorylation of SLP-76 by the ZAP-70 protein-tyrosine kinase is required for T-cell receptor function. J Biol Chem. 1996; 271(33):19641–19644. [PubMed: 8702662]

52. Heyeck SD, Wilcox HM, Bunnell SC, Berg LJ. Lck phosphorylates the activation loop tyrosine of the Itk kinase domain and activates Itk kinase activity. Journal of Biological Chemistry. 1997; 272(40):25401–25408. [PubMed: 9312162]

53. Salcini AE, McGlade J, Pelicci G, Nicoletti I, Pawson T, Pelicci PG. Formation of Shc-Grb2 complexes is necessary to induce neoplastic transformation by overexpression of Shc proteins. Oncogene. 1994; 9(10):2827–2836. [PubMed: 8084588]

54. Ishihara H, Sasaoka T, Ishiki M, Takata Y, Imamura T, Usui I, Langlois WJ, Sawa T, Kobayashi M. Functional importance of Shc tyrosine 317 on insulin signaling in Rat1 fibroblasts expressing insulin receptors. J Biol Chem. 1997; 272(14):9581–9586. [PubMed: 9083103]

55. Prasad KV, Cai YC, Raab M, Duckworth B, Cantley L, Shoelson SE, Rudd CE. T-cell antigen CD28 interacts with the lipid kinase phosphatidylinositol 3-kinase by a cytoplasmic Tyr(P)-Met-Xaa-Met motif. Proc Natl Acad Sci USA. 1994; 91(7):2834–2838. [PubMed: 8146197]

56. Pages F, Ragueneau M, Rottapel R, Truneh A, Nunes J, Imbert J, Olive D. Binding of phosphatidylinositol-3-OH kinase to CD28 is required for T-cell signalling. Nature. 1994; 369(6478):327–329. [PubMed: 8183372]

57. Sadra A, Cinek T, Arellano JL, Shi J, Truitt KE, Imboden JB. Identification of tyrosine phosphorylation sites in the CD28 cytoplasmic domain and their role in the costimulation of Jurkat T cells. J Immunol. 1999; 162(4):1966–1973. [PubMed: 9973466]

58. Teng JM, King PD, Sadra A, Liu X, Han A, Selvakumar A, August A, Dupont B. Phosphorylation of each of the distal three tyrosines of the CD28 cytoplasmic tail is required for CD28-induced T cell IL-2 secretion. Tissue Antigens. 1996; 48(4 Pt 1):255–264. [PubMed: 8946678]

59. Warfel NA, Niederst M, Newton AC. Disruption of the interface between the pleckstrin homology (PH) and kinase domains of Akt protein is sufficient for hydrophobic motif site phosphorylation in the absence of mTORC2. J Biol Chem. 2011; 286(45):39122–39129. [PubMed: 21908613]

60. Kim JH, Xu C, Keum YS, Reddy B, Conney A, Kong AN. Inhibition of EGFR signaling in human prostate cancer PC-3 cells by combination treatment with beta-phenylethyl isothiocyanate and curcumin. Carcinogenesis. 2006; 27(3):475–482. [PubMed: 16299382]

61. Lau C, Wang X, Song L, North M, Wiehler S, Proud D, Chow CW. Syk associates with clathrin and mediates phosphatidylinositol 3-kinase activation during human rhinovirus internalization. J Immunol. 2008; 180(2):870–880. [PubMed: 18178826]

62. King PD, Sadra A, Teng JM, Xiao-Rong L, Han A, Selvakumar A, August A, Dupont B. Analysis of CD28 cytoplasmic tail tyrosine residues as regulators and substrates for the protein tyrosine kinases, EMT and LCK. Journal of immunology (Baltimore, Md : 1950). 1997; 158(2):580–590.

63. Bunnell SC, Diehn M, Yaffe MB, Findell PR, Cantley LC, Berg LJ. Biochemical interactions integrating Itk with the T cell receptor-initiated signaling cascade. J Biol Chem. 2000; 275(3): 2219–2230. [PubMed: 10636929]

64. Fischer KD, Kong YY, Nishina H, Tedford K, Marengere LE, Kozieradzki I, Sasaki T, Starr M, Chan G, Gardener S, Nghiem MP, Bouchard D, Barbacid M, Bernstein A, Penninger JM. Vav is a regulator of cytoskeletal reorganization mediated by the T-cell receptor. Current biology : CB. 1998; 8(10):554–562. [PubMed: 9601639]

65. Hardwick JS, Sefton BM. Activation of the Lck Tyrosine Protein-Kinase by Hydrogen-Peroxide Requires the Phosphorylation of Tyr-394. Proceedings of the National Academy of Sciences of the United States of America. 1995; 92(10):4527–4531. [PubMed: 7538674]

66. Magnan A, Di Bartolo V, Mura AM, Boyer C, Richelme M, Lin YL, Roure A, Gillet A, Arrieumerlou C, Acuto O, Malissen B, Malissen M. T cell development and T cell responses in mice with mutations affecting tyrosines 292 or 315 of the ZAP-70 protein tyrosine kinase. J Exp Med. 2001; 194(4):491–505. [PubMed: 11514605]

67. Chow LM, Fournel M, Davidson D, Veillette A. Negative regulation of T-cell receptor signalling by tyrosine protein kinase p50csk. Nature. 1993; 365(6442):156–160. [PubMed: 8371758]

68. Stefanova I, Hemmer B, Vergelli M, Martin R, Biddison WE, Germain RN. TCR ligand discrimination is enforced by competing ERK positive and SHP-1 negative feedback pathways. Nat Immunol. 2003; 4(3):248–254. [PubMed: 12577055]

69. Saito T, Yokosuka T, Hashimoto-Tane A. Dynamic regulation of T cell activation and co-stimulation through TCR-microclusters. FEBS Lett. 2010; 584(24):4865–4871. [PubMed: 21110974]

70. Miletic AV, Graham DB, Sakata-Sogawa K, Hiroshima M, Hamann MJ, Cemerski S, Kloeppel T, Billadeau DD, Kanagawa O, Tokunaga M, Swat W. Vav links the T cell antigen receptor to the actin cytoskeleton and T cell activation independently of intrinsic Guanine nucleotide exchange activity. PLoS One. 2008; 4(8)

71. Sylvain NR, Nguyen K, Bunnell SC. Vav1-mediated scaffolding interactions stabilize SLP-76 microclusters and contribute to antigen-dependent T cell responses. Sci Signal. 2011; 4(163) ra14.

72. Pauker MH, Hassan N, Noy E, Reicher B, Barda-Saad M. Studying the dynamics of SLP-76, Nck, and Vav1 multimolecular complex formation in live human cells with triple-color FRET. Sci Signal. 2012; 5(221) rs3.

73. Wu J, Motto DG, Koretzky GA, Weiss A. Vav and SLP-76 interact and functionally cooperate in IL-2 gene activation. Immunity. 1996; 4(6):593–602. [PubMed: 8673706]

74. Fang N, Koretzky GA. SLP-76 and Vav function in separate, but overlapping pathways to augment interleukin-2 promoter activity. J Biol Chem. 1999; 274(23):16206–16212. [PubMed: 10347175]

75. Tybulewicz VL. Vav-family proteins in T-cell signalling. Curr Opin Immunol. 2005; 17(3):267–274. [PubMed: 15886116]

76. Bustelo XR. Vav proteins, adaptors and cell signaling. Oncogene. 2001; 20(44):6372–6381. [PubMed: 11607839]

77. Lazer G, Pe'er L, Farago M, Machida K, Mayer BJ, Katzav S. Tyrosine residues at the carboxyl terminus of Vav1 play an important role in regulation of its biological activity. The Journal of biological chemistry. 2010; 285(30):23075–23085. [PubMed: 20457609]

78. Kosugi A, Sakakura J, Yasuda K, Ogata M, Hamaoka T. Involvement of SHP-1 tyrosine phosphatase in TCR-mediated signaling pathways in lipid rafts. Immunity. 2001; 14(6):669–680. [PubMed: 11420038]

79. Kon-Kozlowski M, Pani G, Pawson T, Siminovitch KA. The tyrosine phosphatase PTP1C associates with Vav, Grb2, and mSos1 in hematopoietic cells. J Biol Chem. 1996; 271(7):3856–3862. [PubMed: 8632004]

80. Pani G, Fischer KD, Mlinaric-Rascan I, Siminovitch KA. Signaling capacity of the T cell antigen receptor is negatively regulated by the PTP1C tyrosine phosphatase. J Exp Med. 1996; 184(3): 839–852. [PubMed: 9064344]

81. Stebbins CC, Watzl C, Billadeau DD, Leibson PJ, Burshtyn DN, Long EO. Vav1 dephosphorylation by the tyrosine phosphatase SHP-1 as a mechanism for inhibition of cellular cytotoxicity. Mol Cell Biol. 2003; 23(17):6291–6299. [PubMed: 12917349]

82. Kim JE, White FM. Quantitative analysis of phosphotyrosine signaling networks triggered by CD3 and CD28 costimulation in Jurkat cells. J Immunol. 2006; 176(5):2833–2843. [PubMed: 16493040]

83. Boomer JS, Green JM. An enigmatic tail of CD28 signaling. Cold Spring Harb PerspectBiol. 2010; 2(8):a002436.

84. Kim HH, Tharayil M, Rudd CE. Growth factor receptor-bound protein 2 SH2/SH3 domain binding to CD28 and its role in co-signaling. J Biol Chem. 1998; 273(1):296–301. [PubMed: 9417079]

85. Raab M, Cai YC, Bunnell SC, Heyeck SD, Berg LJ, Rudd CE. p56Lck and p59Fyn regulate CD28 binding to phosphatidylinositol 3-kinase, growth factor receptor-bound protein GRB-2, and T cell-specific protein-tyrosine kinase ITK: implications for T-cell costimulation. Proc Natl Acad Sci USA. 1995; 92(19):8891–8895. [PubMed: 7568038]

86. Schneider H, Cai YC, Prasad KV, Shoelson SE, Rudd CE. T cell antigen CD28 binds to the GRB-2/SOS complex, regulators of p21ras. Eur J Immunol. 1995; 25(4):1044–1050. [PubMed: 7737275]

87. Collins TL, Deckert M, Altman A. Views on Vav. Immunol Today. 1997; 18(5):221–225. [PubMed: 9153953]

88. Fischer KD, Tedford K, Penninger JM. Vav links antigen-receptor signaling to the actin cytoskeleton. Semin Immunol. 1998; 10(4):317–327. [PubMed: 9695188]

89. Hornstein I, Alcover A, Katzav S. Vav proteins, masters of the world of cytoskeleton organization. Cell Signal. 2004; 16(1):1–11. [PubMed: 14607270]

90. Tavano R, Contento RL, Baranda SJ, Soligo M, Tuosto L, Manes S, Viola A. CD28 interaction with filamin-A controls lipid raft accumulation at the T-cell immunological synapse. Nat Cell Biol. 2006; 8(11):1270–1276. [PubMed: 17060905]

91. al-Shami A, Bourgoin SG, Naccache PH. Granulocyte-macrophage colony-stimulating factor-activated signaling pathways in human neutrophils. I. Tyrosine phosphorylation-dependent stimulation of phosphatidylinositol 3-kinase and inhibition by phorbol esters. Blood. 1997; 89(3): 1035–1044. [PubMed: 9028336]

92. Shigematsu H, Iwasaki H, Otsuka T, Ohno Y, Arima F, Niho Y. Role of the vav proto-oncogene product (Vav) in erythropoietin-mediated cell proliferation and phosphatidylinositol 3-kinase activity. J Biol Chem. 1997; 272(22):14334–14340. [PubMed: 9162069]

93. Ramos-Morales F, Druker BJ, Fischer S. Vav binds to several SH2/SH3 containing proteins in activated lymphocytes. Oncogene. 1994; 9(7):1917–1923. [PubMed: 8208538]

94. Welch HC, Coadwell WJ, Stephens LR, Hawkins PT. Phosphoinositide 3-kinase-dependent activation of Rac. FEBS Lett. 2003; 546(1):93–97. [PubMed: 12829242]

A

B
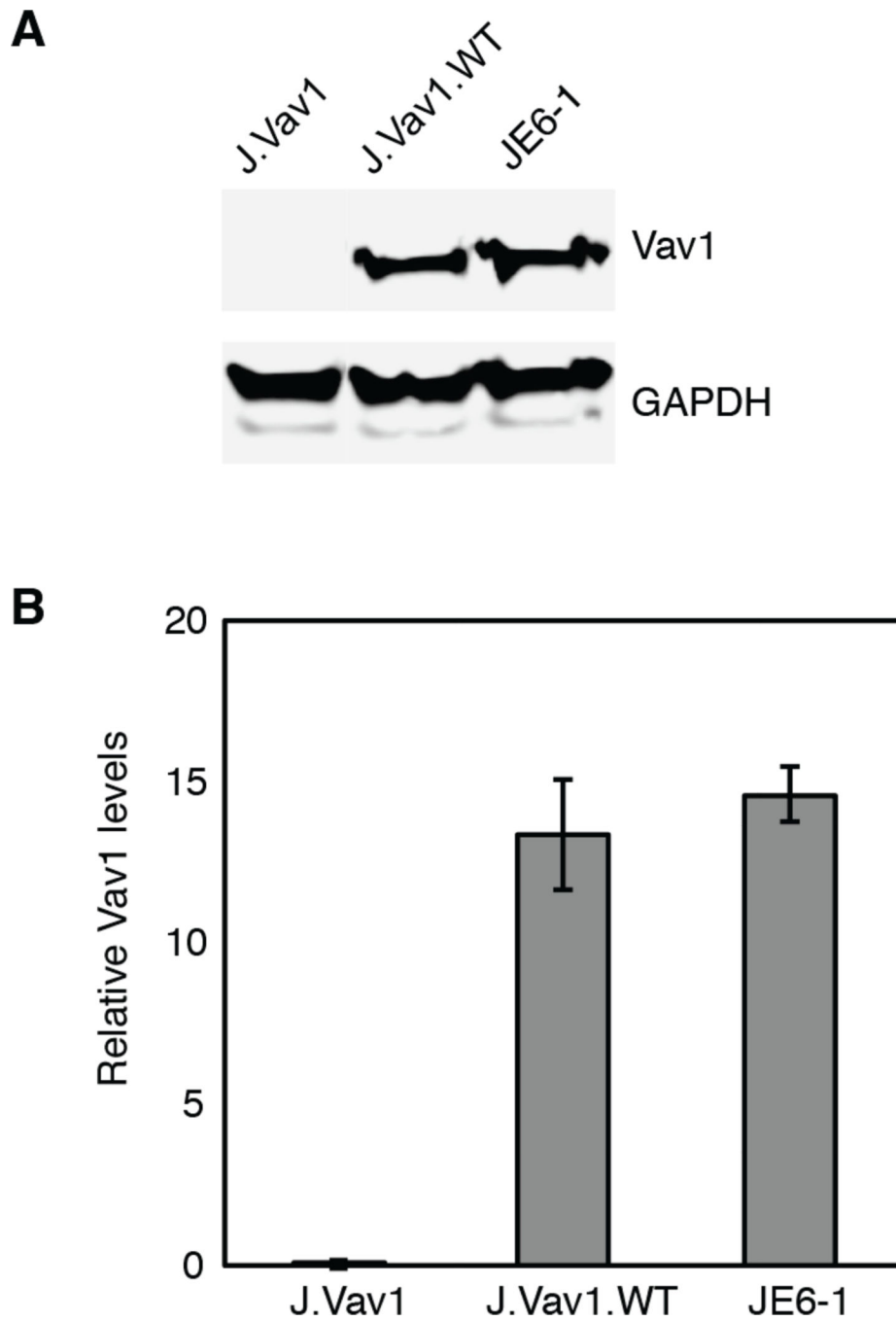
Figure 1. Vav1 expression in J.Vav1 and J.Vav1.WT cells
A) J.Vav1, J.Vav1.WT, and Jurkat T cell (JE6-1) lysates were analyzed by Western blotting for Vav1 and GAPDH. B) Densitometric analysis of Vav1 levels normalized to GAPDH levels was performed. Shown is the mean ± S.D. from three biological replicate experiments.
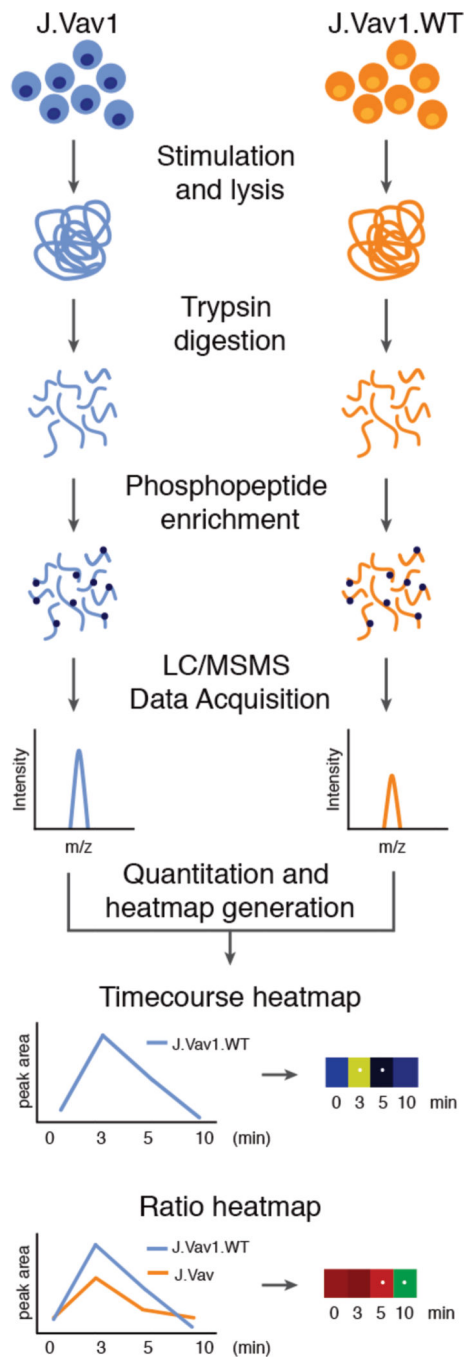
Figure 2. Experimental strategy

J.Vav1 and J.Vav1.WT cells were pre-incubated with OKT3 and OKT4 antibodies for 30 seconds at 37°C and then cross-linked with IgG at 37°C for 0, 3, 5, and 10 minutes. Subsequent to lysis, samples were digested into peptides and enriched for phosphopeptides. Phosphopeptides from 5 biological replicates were identified using LC-MS/MS analysis and the resulting SIC peak areas of phosphopeptides from J.Vav1 and J.Vav1.WT cells were quantified. Temporal heatmaps were generated from the replicate average peak areas of each phosphopeptide across the time course of TCR stimulation. Ratio heatmaps were generated

by taking the ratio of average replicate peak areas of J.Vav1 and J.Vav1.WT cells for each time point and phosphopeptide.
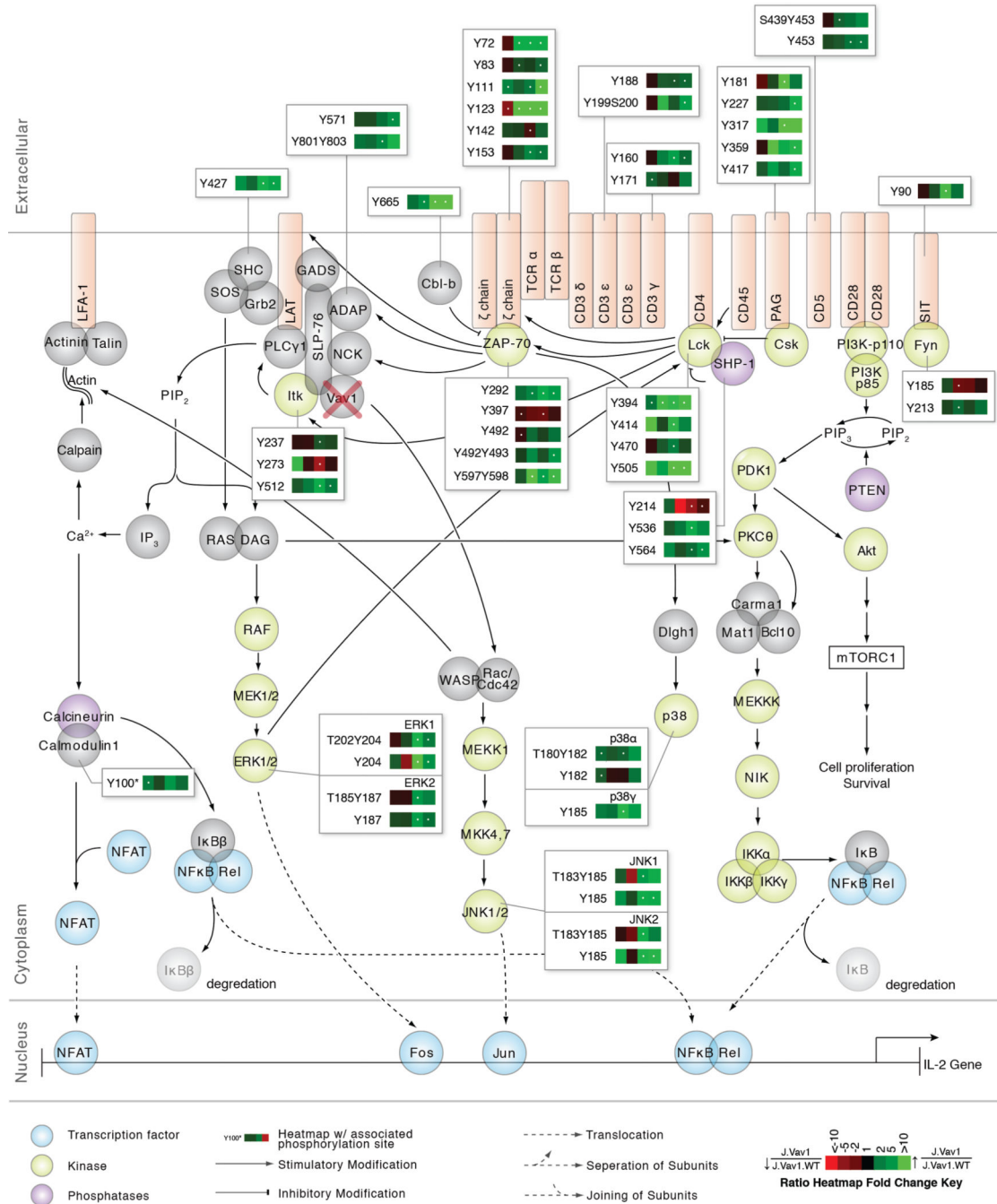
Figure 3. Vav1 deficiency results in elevated phosphorylation on canonical TCR signaling proteins

Depicted is the canonical TCR signaling pathway with quantitative J.Vav1 to J.Vav1.WT ratio heatmaps beside individual proteins, corresponding to the changes in phosphorylation between the two cell types across the four time points of TCR stimulation. Heatmaps were calculated from the average of five biological replicate experiments. Green represents elevated phosphorylation in J.Vav1 cells relative to J.Vav1.WT cells, whereas red represents decreased phosphorylation in J.Vav1 cells relative to J.Vav1.WT cells according to the figure legend. Black represents no change. White dots within the heatmap indicate a
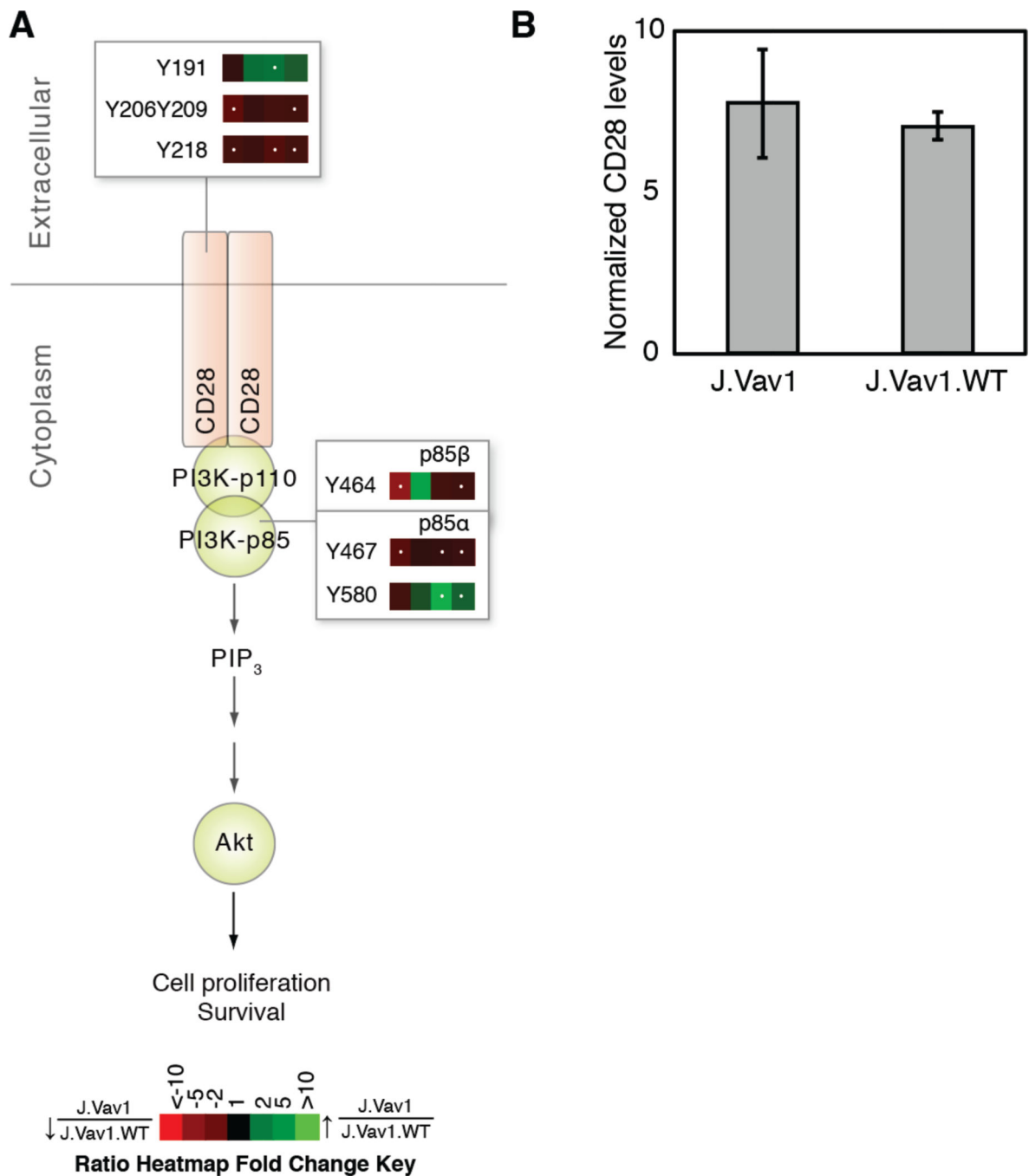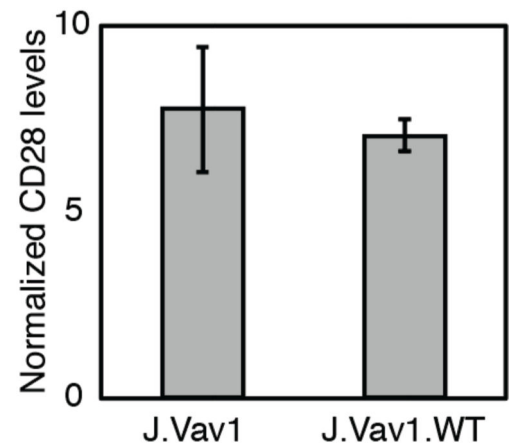
statistically significant difference (q value < 0.05; >1.5-fold or <0.67-fold) for that time point and phosphopeptide across the five biological replicate experiments.

**Figure 4. Vav1 deficiency results in altered phosphorylation on CD28 and PI3K**
A) Ratio heatmaps were calculated from the average of five biological replicate experiments comparing J.Vav1 to J.Vav1.WT across four time points of TCR stimulation. White dots within the heatmap indicate a statistically significant difference (q value < 0.05; >1.5-fold or <0.67-fold) for that time point and phosphopeptide. B) J.Vav1 and J.Vav1.WT lysates were analyzed by Western blotting for CD28 and COX IV. Densitometric analysis of CD28 levels normalized to COX IV levels was performed. Shown is the mean ± S.D. from five biological replicate experiments.
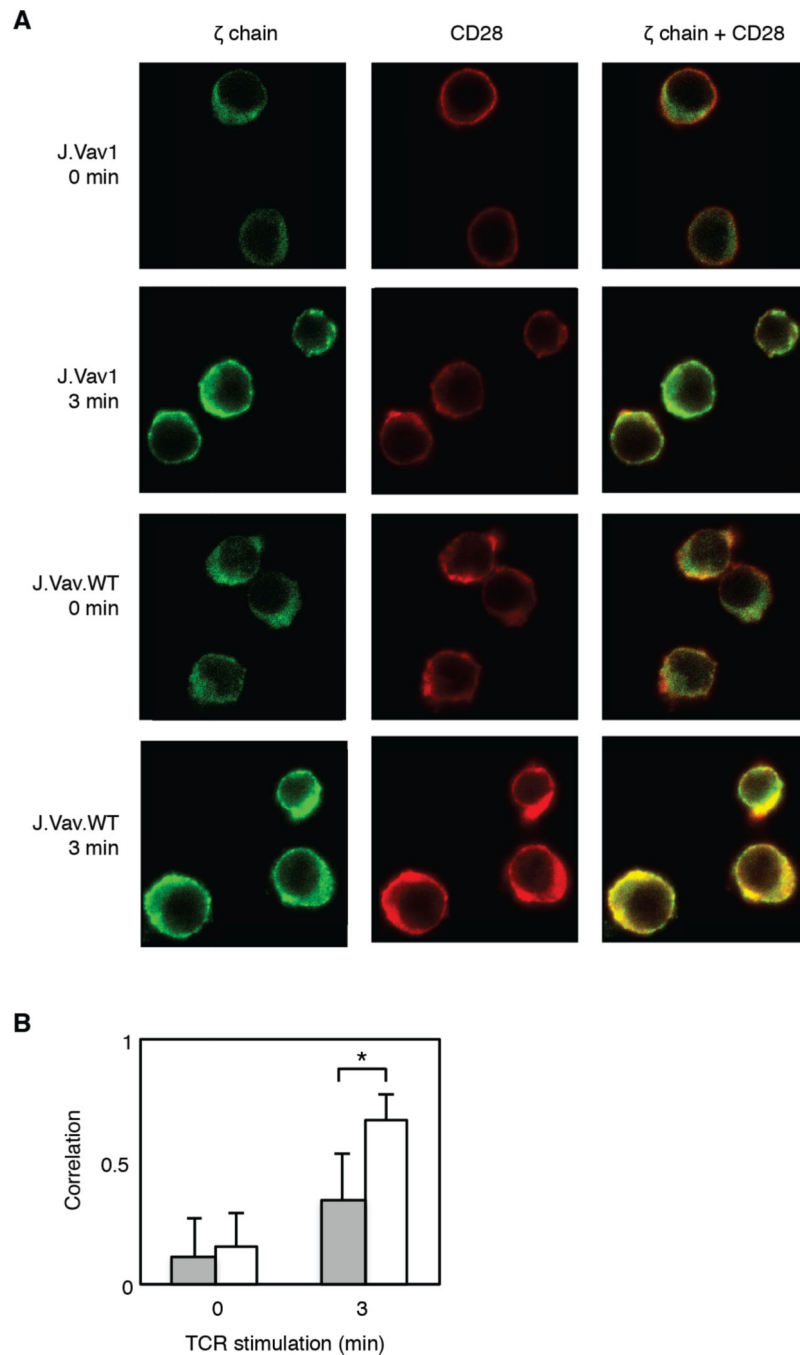
Figure 5. Colocalization of CD28 and ζ chain of the TCR is attenuated in Vav1-deficient T cells
J.Vav1 and J.Vav1.WT cells stimulated for either 0 or 3 minutes were fixed and analyzed by confocal microscopy. Cells were labeled with goat anti-CD28 and mouse anti-ζ chain, washed, and subsequently labeled with the secondary antibodies Alexa Fluor 488 donkey anti-mouse and Alexa Fluor 647 donkey anti-goat. A) CD28 is represented in red and ζ chain is represented in green. Colocalized CD28 and ζ chain is shown in yellow. B) Colocalization was quantified using the ZEN software in which colocalization coefficients, derived from the Pearson's correlation coefficient, were calculated. Gray bars represents

J.Vav1 cells and white bars represents J.Vav1.WT cells. Shown is the mean ± S.D. from 75 cells for each cell type and time point. Student t-tests identified statistically significant differences in colocalization between stimulated J.Vav1 and J.Vav1.WT cells (*-p value < 1×10^{-9}).
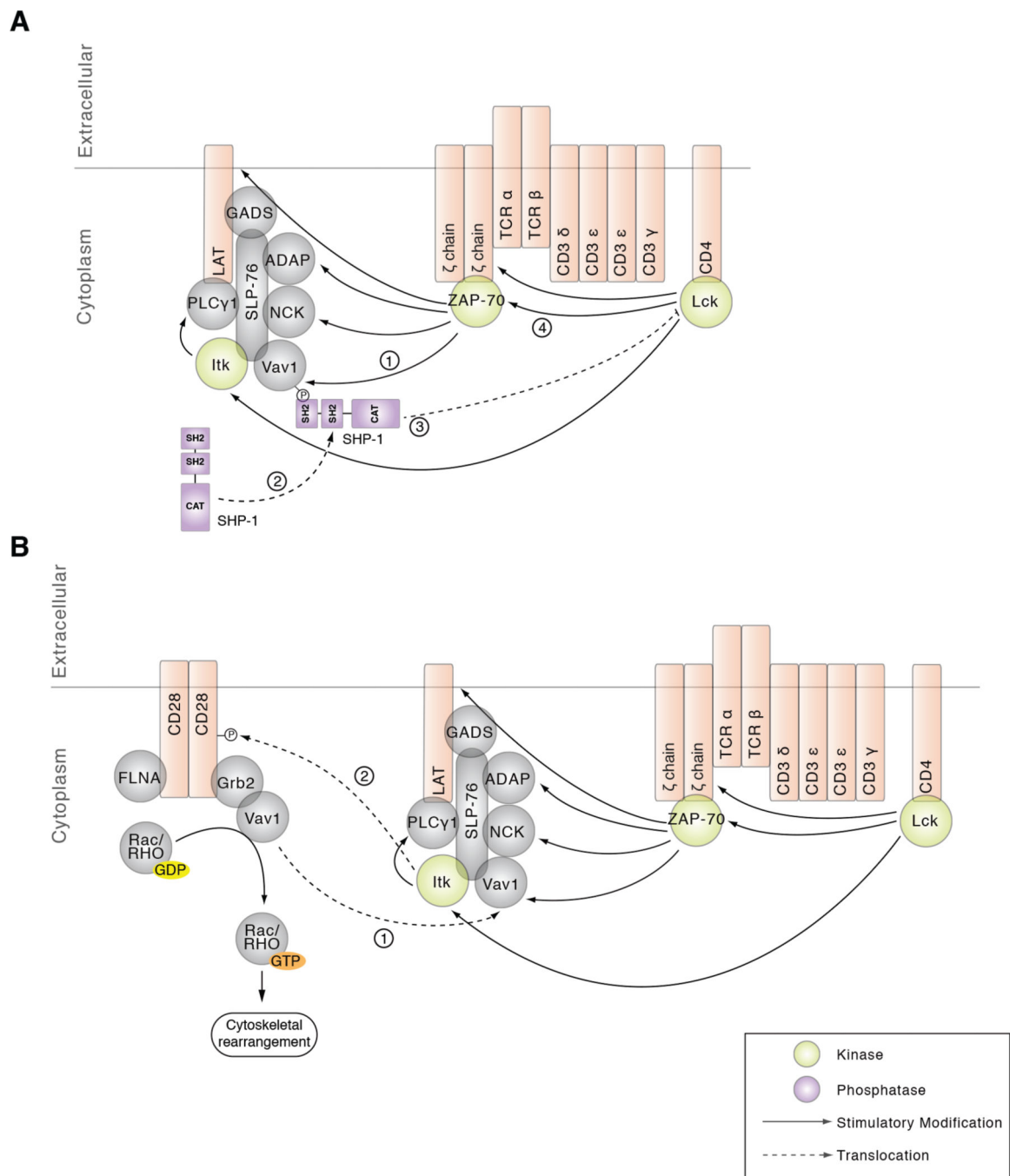
Figure 6. Proposed models for Vav1 mediated regulation of TCR signaling
A) Phosphorylation of Vav1 recruits the tyrosine phosphatase SHP-1, which regulates Lck activity, as well as the CD3 and ζ ITAMs and ZAP-70, substrates of Lck. B) CD28 recruitment to the TCR may be mediated via Vav1 association with Grb2. Additionally, Vav1 regulates rearrangements of the cytoskeleton that may be necessary for CD28 localization to the TCR.